JOURNAL OF THERMOPHYSICS AND HEAT TRANSFER
Vol. 9, No. 2, April–June 1995

Numerical Solutions to Nozzle Flows with Vibrational Nonequilibrium

V. Babu* and V. V. Subramaniam†
Ohio State University, Columbus, Ohio 43210

In many applications of reacting flows including the modeling of gas lasers, there is a great need to couple finite rate kinetics with the governing conservation equations for the flow. This problem is particularly acute in the case of multidimensional reacting flows due to the additional stringent demands of computational speed, efficiency, and accuracy. In this article, numerical solutions to quasi-one-dimensional supersonic flows in nozzles with large area variation and state-specific vibrational rate kinetics are presented. The present formulation, unlike previous formulations is more general and the numerical method used here extends easily to two and three dimensions. Boundary and initial conditions are discussed and these extend to multidimensions easily as well. Results obtained using the present method are compared with those reported in Chiroux de Gavelle de Roany et al. (*AIAA Journal*, Vol. 31, No. 1, 1993, pp. 119–128), as illustrative examples.

Nomenclature

A = cross-sectional area of the nozzle, m^2
$E_{i,v}$ = energy of vibrational level v of species i, J
e = internal energy per unit volume, J/m^3
k = Boltzmann's constant, J/K
$M_{i,v}$ = molecular mass of the diatomic species, kg
M_m = atomic or molecular mass of the diluent species, kg
N_d = number of vibrationally active species
N_m = number of diluent species
$n_{i,v}$ = number density of vibrationally active species i in level v where v is the vibrational quantum number, m^{-3}
n_m = number density of diluent species m, m^{-3}
p = pressure, N/m^2
p_0 = reservoir pressure, N/m^2
T = temperature, K
T_0 = reservoir temperature, K
t = time, s
u = velocity, m/s
$V_{\max}$ = highest vibrational level considered in the diatomic species
x = axial or streamwise coordinate, m
ρ = mass density, kg/m^3

I. Introduction

IN the measurement of chemical rate constants or studies of high-temperature chemistry, shock tubes are used. Often, supersonic nozzles are added to the ends of the shock tube to "freeze" large amounts of energy in the internal degrees of freedom (DOF) of molecules, so that these states can be interrogated further downstream. These reacting and nonequilibrium flows are in most cases at least two dimensional in nature, so that significant gradient in concentrations can exist. Inference of rates from experimental measurements is therefore difficult to make unless there is an accompanying numerical model of the chemical kinetics incorporating the gas flow dynamics.

Recently, numerical solutions to supersonic nozzle flows with a high degree of vibrational nonequilibrium and state-specific kinetics have been presented.[1] These quasi-one-dimensional solutions were obtained by integrating the steady forms of the governing equations using the stiff differential equation integrator LSODE.[2] In this article, we extend the work of Chiroux de Gavelle de Roany et al.[1] in two respects; one concerns the formulation of the problem, and the second utilizes a numerical method different from that used in their work. In their formulation, Chiroux de Gavelle de Roany et al. assume that the average molecular weight remains constant along the entire length of the nozzle. While this assumption was justified for the cases that they considered and greatly simplifies the problem, it is generally not valid in chemically reacting flows. The formulation that we present in the next section does not require the average molecular weight to be constant. Although we do not present solutions for chemically reacting flows, the formulation extends equally as well to such flows. The second point concerns the use of LSODE for obtaining numerical solutions for nonequilibrium flows. While it is possible to obtain solutions to one-dimensional problems with LSODE, it does not extend to multiple dimensions. This is a serious drawback if one wants to study such flows in two and three dimensions, while including the effects of heat conduction and viscosity. Hence, it is desirable to have a numerical method that can handle such stiff problems with the potential to extend from one dimension all the way to three dimensions. We recently[3] showed that the linearized block implicit (LBI) scheme of Briley and McDonald[4] is very well-suited for studying one- and two-dimensional axisymmetric, plasma flows in geometries with large exit-to-throat area ratios. In this article, we show the suitability of this method for studying nonequilibrium flows by applying it to some of the same problems considered in Chiroux de Gavelle de Roany et al.[1]

This article is organized as follows. Formulation of the problem is discussed in Sec. II, followed by a discussion of the numerical method in Sec. III. Finally, some illustrative examples and a brief discussion of the results are given in Sec. IV.

II. Formulation

The governing equations are the quasi-one-dimensional gas dynamic equations together with species conservation equations.[1] We consider the governing equations in their unsteady form here. These can be written as follows:

$$\frac{\partial \rho}{\partial t} + \frac{1}{A}\frac{\partial(\rho u A)}{\partial x} = 0 \tag{1}$$

Received March 7, 1994; revision received Aug. 15, 1994; accepted for publication Sept. 22, 1994.

*Post-Doctoral Research Associate, Department of Mechanical Engineering. Member AIAA.
†Associate Professor, Department of Mechanical Engineering. Member AIAA.

$$\frac{\partial(\rho u)}{\partial t} + \frac{1}{A}\frac{\partial(\rho u^2 A)}{\partial x} = -\frac{\partial p}{\partial x} \tag{2}$$

$$\frac{\partial}{\partial t}\left(e + \frac{\rho u^2}{2}\right) + \frac{1}{A}\frac{\partial}{\partial x}\left[uA\left(e + p + \frac{\rho u^2}{2}\right)\right] = 0 \tag{3}$$

$$\frac{\partial n_{i,v}}{\partial t} + \frac{1}{A}\frac{\partial(n_{i,v} uA)}{\partial x} = VT_{i,v} + VV_{i,v} + SRD_{i,v}$$
$$1 \le i \le N_d, \qquad 0 \le v \le V_{\max} \tag{4}$$

$$\frac{\partial n_m}{\partial t} + \frac{1}{A}\frac{\partial(n_m uA)}{\partial x} = 0, \qquad 1 \le m \le N_m \tag{5}$$

where the subscripts i, v refer to diatomic species i in vibrational state v, and the subscript m refers to diluent species (usually monatomic). In addition, only the diatomic species are assumed to be vibrationally active, and $V_{\max} + 1$ is the total number of vibrational levels considered in each of the diatomic species. $E_{i,v}$ is calculated by treating the diatomic molecules as anharmonic oscillators.[1] The heat of formation of various species can be included in the energy equation. However, since chemical reactions are not considered in the examples presented here, they have been left out of Eq. (3). Also, energy of the electronic levels is neglected because we do not include electronic transitions in the examples. The radiative loss that would appear as a sink term on the right side of Eq. (3) is neglected here since it is expected to be small for the optically thin gases considered. These assumptions do not indicate a loss of generality, since all these terms can be included in the formulation if applicable. The terms on the right side of Eq. (4) represent the state-specific vibration-translation (VT), vibration-vibration (VV), and spontaneous radiative decay (SRD) terms as described in the Appendix.

The pressure is related to the temperature and the number densities through the following equation of state:

$$p = \left(\sum_{i=1}^{N_d}\sum_{v=0}^{V_{\max}} n_{i,v} + \sum_{m=1}^{N_m} n_m\right) kT \tag{6}$$

where k is Boltzmann's constant ($=1.38 \times 10^{-23}$ J/K), and the mass density is related to the number densities as follows:

$$\rho = \sum_{i=1}^{N_d}\sum_{v=0}^{V_{\max}} M_i n_{i,v} + \sum_{m=1}^{N_m} M_m n_m \tag{7}$$

where M stands for the atomic or molecular mass of the respective species. The internal energy per unit volume is given by the following—assuming equilibrium between the translational and rotational modes:

$$e = \frac{3}{2}kT\sum_{m=1}^{N_m} n_m + \sum_{i=1}^{N_d}\sum_{v=0}^{V_{\max}} n_{i,v}\left(\frac{5}{2}kT + E_{i,v}\right) \tag{8}$$

We assume that a large reservoir is present upstream of the nozzle and that the conditions in the reservoir such as temperature, pressure, and volume fractions of the various species present are known. Furthermore, it is assumed that the diatomic species are in Boltzmann equilibrium, both in the reservoir and at the nozzle inlet plane, and that the mixture is compositionally frozen between these two locations. In addition, heat losses and frictional losses going from the reservoir to the nozzle inlet are assumed to be negligible, without any loss of generality. These assumptions correctly describe the inlets in shock tube systems that are typically used to study high-temperature chemistry.

With the above assumptions, we can relate the conditions at the nozzle inlet to those at the reservoir by conservation of energy. This gives us an equation that involves the velocity, temperature, and total number density ($=\sum_{i=1}^{N_d}\sum_{v=0}^{V_{\max}} n_{i,v} + \sum_{m=1}^{N_m} n_m$) at the inlet. Since the volume fractions of the monatomic species at the inlet are known, we can relate the individual n_m to the total number density. For the diatomic species, the known volume fractions at the inlet, together with the fact that they are in Boltzmann equilibrium,[5] allows us to relate the $n_{i,v}$ to the total number density. Finally, we can relate the inlet static pressure, and hence, the total number density [see Eq. (6)], and temperature to their respective values at the reservoir through the isentropic equation of state.[6] In the present case, the velocity at the inlet of the nozzle is small (about 6 m/s or so) because of the large inlet-to-throat area ratio, and thus, the use of the isentropic equation of state is acceptable. These conditions allow us to eliminate all the dependent variables except the velocity at the inlet, which is determined through an implicit extrapolation.[4] At the exit to the nozzle, implicit extrapolation is used for all the variables[3] since we are interested only in supersonic flows.

Although the governing equations and boundary conditions have been presented in their dimensional form in this section, it must be pointed out that they are nondimensionalized before being solved numerically. This we do by using upstream reservoir conditions as reference quantities. This choice is especially convenient, since the reservoir conditions need to be specified as boundary conditions, as we have already seen.

III. Numerical Method

Equations (1–5), together with the boundary conditions, are discretized in time and linearized implicitly using the procedure outlined by Briley and McDonald.[4] Artificial dissipation in the form of a second derivative in the axial or streamwise coordinate is added to the right side of Eqs. (1–5) to ensure numerical stability.[4] These equations are then discretized using second-order accurate central differences on a nonuniform grid with fine spacings near the throat region. After eliminating the boundary points from the resulting system of linear algebraic equations using the boundary conditions, a block tridiagonal system of equations results that can be solved by using standard block LU decomposition algorithms.[7] We must note at this point that this system is linearly dependent due to the relationship between ρ and the number densities through Eq. (7), which hold at each grid point. In order to make this system linearly independent, we arbitrarily replace one of the species equations, such as the one corresponding to $i = 1$ and $v = 0$ at each grid point, with Eq. (7) applied at that grid point. Note that this is done implicitly so that overall stability is not lost. The system of equations is now rendered linearly independent and is ready to be solved.

Since we are solving the unsteady form of the governing equations, the frozen flow solution is prescribed as the initial guess to start the solution process. This solution is obtained by numerically solving the above system of equations with the right side of Eq. (4) set identically to zero. In principle, a truly frozen flow cannot be used as an initial guess for nonequilibrium calculations. However, in practice, these solutions exhibit deviations from the truly frozen flow solution due to discretization and round-off errors normally present in such numerical solutions. Therefore, the frozen flow solution can be used as an initial guess for the nonequilibrium calculations.

IV. Illustrative Examples and Discussion

As illustrative examples, we consider some of the cases from Chiroux de Gavelle de Roany et al.[1] This nozzle has a rectangular cross section and is composed of two sections—a section with a quadratically varying area followed by one in which the area varies linearly with a slope equal to 15 deg.

The total length of the nozzle is 1 m, and its width perpendicular to the page is 0.01 m. The variation of the height transverse to the flow (in m) vs the axial coordinate is

$$h(x) = 2(2376x^2 + 0.0024), \quad -0.01 \le x \le x_t$$

$$h(x) = 2[0.0024 + 2376x_t^2 + (x - x_t)\tan 15]$$

$$x_t \le x \le 0.99$$

where $x_t = 5.64 \times 10^{-5}$ m. The nozzle has an inlet-to-throat area ratio of 100, and an exit-to-throat area ratio of approximately 111. For all the results presented here, a total of 100 grid points is used in the axial direction. The grid is nonuniform[8] with a finest spacing of 0.00072 m at the throat region. The unsteady, nonequilibrium calculations are stopped when the percent change in the variables is less than or equal to 0.00001%. Since the number of grid points is the same for all the cases, the total computing time for each case depends almost entirely upon the size of the blocks in the block tridiagonal system, which is equal to $3 + N_m + N_d(V_{\max} + 1)$. In the present study, block sizes as large as 86 (corresponding to $N_m = 1$, $N_d = 2$, and $V_{\max} = 40$) are considered. The total computing time (including the time taken for generating the initial guess) for the case of largest block size is about 15–20 min in the uniprocessor mode on the Cray Y-MP, whereas it is about 10 min for the cases with a single diatomic species. For all the examples presented in this section, the reservoir temperature and pressure are kept at 2000 K and 100 atm, respectively.

The first case is a flowing mixture of CO, Ar, and H_2. The volume fraction of CO is kept constant at 20%, whereas the volume fraction of Ar is varied from a baseline value of 80% corresponding to 0% H_2, up to 70% corresponding to 10% H_2. It must be pointed out that only the CO is treated as being vibrationally active. The H_2 is simply treated as a molecular diluent participating only in VT transfer. The vibrational population distributions of CO at the nozzle exit plane for 0, 1, and 10% H_2 in the mixture are shown in Fig. 1. As can be seen from these distributions, V-T relaxation of CO by H_2 is significant for increasing percentages of H_2 in the mixture. The population distributions, however, are not as sensitive to small changes in the percentages of H_2 as was reported by Chiroux de Gavelle de Roany et al.[1] This is due to an error in the values of the constants $A_{j,k}$, $B_{j,k}$ and $C_{j,k}$ (see Table 1 in Ref. 1) used for calculating the CO-H_2 V-T rates. These constants are obtained by fitting the rate expressions to the experimental values of the $v = 1 \rightarrow v = 0$ transition rates of CO-H_2 reported by Poulsen and Billing.[9] The correct values for these constants (which are used in this work), are $A_{j,k} = 6.0001$, $B_{j,k} = -10.4149$, and $C_{j,k} = -13.4749$. Our conclusions are supported by optical pumping experiments reported by Straub.[10]

The second example that we consider is the flow of a 20% CO-20% N_2-60% Ar mixture with the same reservoir conditions as before. In this case, both CO and N_2 are vibrationally active. The vibrational populations of these species at the exit plane are plotted in Fig. 2. The distributions show considerable nonequilibrium, and the number densities of N_2 for vibrational levels above 5 are about 6 orders of magnitude lower than those of CO. These distributions agree very well qualitatively and somewhat quantitatively with those pre-

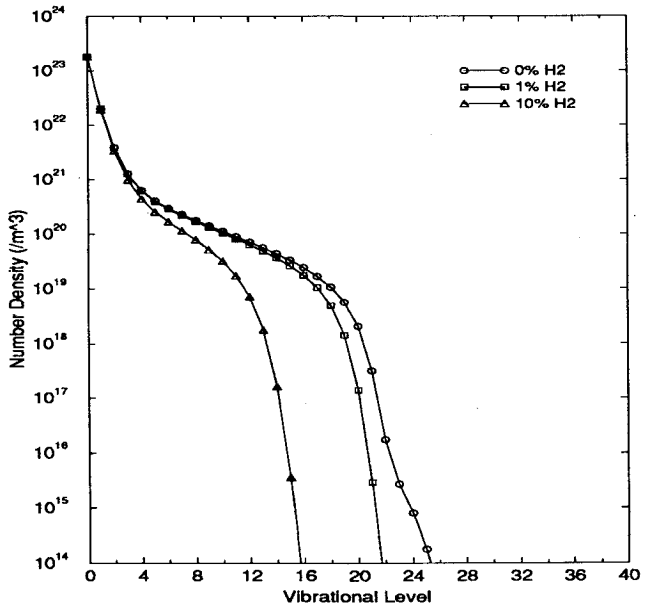

Fig. 1 Vibrational population distribution of CO at the exit of the nozzle for the flow of CO-Ar-H_2 mixtures with $T_0 = 2000$ K and $p_0 = 100$ atm.

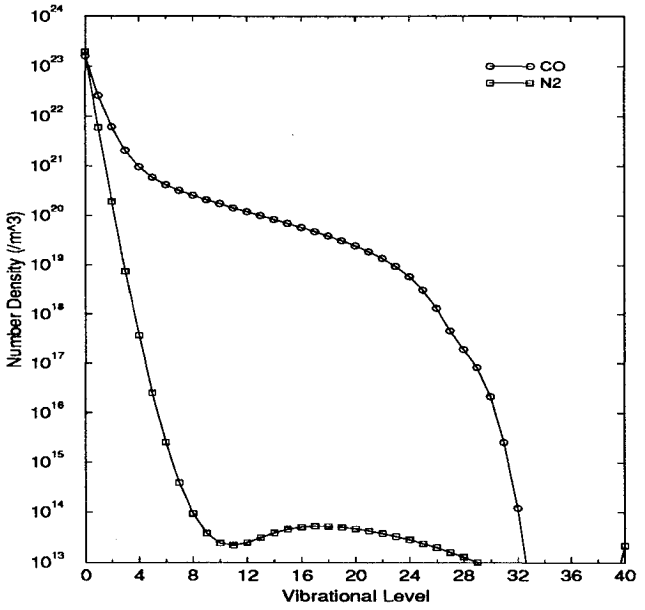

Fig. 2 Vibrational population distributions of CO and N_2 at the exit of the nozzle for the flow of a CO-Ar-N_2 mixture with $T_0 = 2000$ K and $p_0 = 100$ atm.

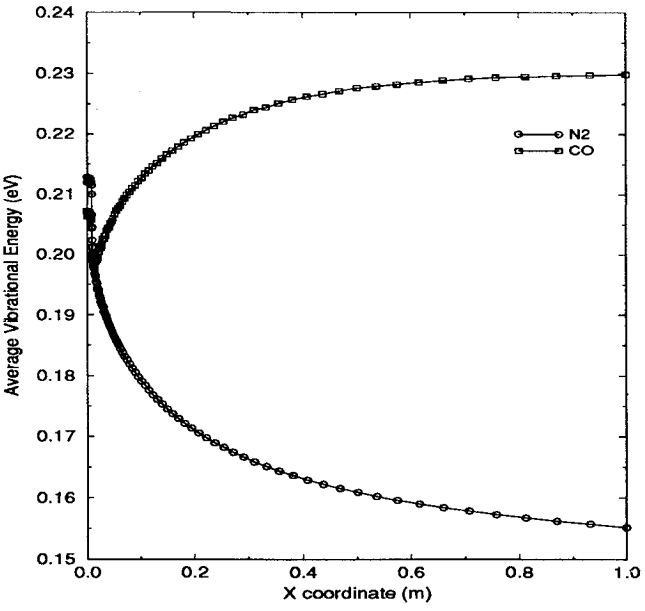

Fig. 3 Plot of the average vibrational energy along the nozzle for the flow of a CO-Ar-N_2 mixture with $T_0 = 2000$ K and $p_0 = 100$ atm.

sented in Ref. 1. The average vibrational energy per species, defined as $\Sigma_{v=0}^{V_{max}} n_{i,v}E_{i,v}/\Sigma_{v=0}^{V_{max}} n_{i,v}$, is plotted in Fig. 3 for CO and N_2. Dramatic transfer of vibrational energy from N_2, which has more widely spaced energy levels, to CO, which has more closely spaced levels, can be seen in this figure. This is in agreement with theoretical predictions[11] as well as with the numerical results presented by Chiroux de Gavelle de Roany et al.[1]

V. Summary and Conclusions

In summary, quasi-one-dimensional solutions including state-specific kinetics for flow exhibiting strong vibrational nonequilibrium in a large area ratio nozzle are presented. These are obtained with the LBI scheme of Briley and McDonald.[4] This algorithm allows the use of nondimensional time steps as large as 0.01 (approximately 10^{-5} s), even in the presence of large stiffness, and can run at computing speeds as high as 250 Mflops in the uniprocessor mode on the Cray Y-MP. Chemical reactions can also be easily included in the present formulation. The LBI method is extendable to two dimensions[4] and three dimensions as well.[12] However, practical constraints on computing resources dictate that the total number of vibrational levels considered per diatomic species be chosen judiciously to make such calculations feasible in two and three dimensions.

Appendix: Summary of Rate Expressions

The detailed expressions for the VT, VV, and the SRD terms are given here. Even though the expressions that are presented look identical to those given by Chiroux de Gavelle de Roany et al.,[1] there are some minor differences between the two due to typographical errors in Chiroux de Gavelle de Roany et al.

$E_{i,v}$ is given by

$$E_{i,v} = \frac{1.6022 \times 10^{-19}}{8065.479}\left[\omega_{ei}\left(v + \frac{1}{2}\right) - \omega_{ei}\chi_{ei}\left(v + \frac{1}{2}\right)^2\right]$$

where the electronic energy has been neglected since we consider only ground electronic states. In general, $E_{i,v}$ is also dependent on the rotational quantum number,[13] but in this work we treat the rotational modes as being in equilibrium with the translational modes. ω_{ei} (in cm^{-1}), and χ_{ei} (dimensionless) are the spectroscopic constants for molecules of species i (see Table A1).

Vibration-Translation Term

The VT term in the species Eq. (4) can be written as

$$VT_{i,v} = \sum_{j=1}^{N_d+N_m} n_j\{P_{i,j}^{v+1,v}[n_{i,v+1} - \exp(-\Delta E_i^v/kT)n_{i,v}]$$

$$- P_{i,j}^{v,v-1}[n_{i,v} - \exp(-\Delta E_i^{v-1}/kT)n_{i,v-1}]\}$$

where

$$n_j = \sum_{w=0}^{V_{max}} n_{j,w}$$

in the case of a vibrationally active species and $n_j = n_m$ in the case of a diluent species. Also, $P_{i,j}^{v,v-1}$ is the rate constant (in m^3/s) of the VT transition:

$$X_i(v) + X_j \rightarrow X_i(v-1) + X_j$$

where $X_i(v)$ refers to species i in vibrational state v. The rate constant is given by[1]

$$P_{i,j}^{v,v-1} = \mathcal{P}_{i,j}[v/(1 - \chi_{ei}v)]F(\lambda_{i,j}^{v,v-1})$$

where

$$F(\psi) = \tfrac{1}{2}(3 - e^{-2\psi/3})e^{-2\psi/3}$$

with

$$\lambda_{i,j}^{v,v-1} = 2^{-3/2}\sqrt{(\alpha_{i,j}/T)}(|\Delta E_i^{v-1}|/k)$$

Here, $\Delta E_i^{v-1} = E_{i,v} - E_{i,v-1}$ is the difference in energy between products and reactants in the VT transition. The quantity $\alpha_{i,j}$ is a parameter that is adjusted to give the best possible fit to the best available experimental rate data (or numerical calculation if no experimental data are available) over different vibrational levels. In cases where no data is available, it is taken to be equal to $\Theta_{i,j}/\Theta_i^2$, where $\Theta_i = hc\omega_{ei}/k$ (with c, the speed of light in cm/s) is the characteristic vibrational temperature (in K) of species i, and $\Theta_{i,j} = 16\pi^4\,\mu_{i,j}c^2\omega_{ei}^2 l^2/k$ is in K, where $\mu_{i,j}$ is the reduced mass in kg and $l\,(=0.2 \times 10^{-10}\text{ m})$ is the range parameter.[14] It should be emphasized at this point that the rate model that is used here is the same as in Ref. 1, even though a new parameter $\alpha_{i,j}$ has been introduced. This is done to clearly bring out the fact that the $\Theta_{i,j}$ used in Ref. 1 (and in the related references cited therein) is a parameter as well, and its value is not always equal to that given by SSH theory.

In the above expression for the rate constant, $\mathcal{P}_{i,j}$ is a coefficient that allows for fitting to the available experimental relaxation data for the 1-0 transition rate, i.e., $P_{i,j}^{1,0}$. It is given (in m^3/s) as

$$\mathcal{P}_{i,j} = \frac{10(1 - \chi_{ei})kT}{(\tau p)_{i,j}F_{i,j}^{1,0}\{1 - \exp[-\Theta_i/(T)]\}}$$

Here, $(\tau p)_{i,j}$ is the vibrational relaxation time in μs.atm, and is expressed as

$$(\tau p)_{i,j} = A_{i,j} + B_{i,j}(T)^{-1/3} + C_{i,j}(T)^{-2/3}$$

where $A_{i,j}$, $B_{i,j}$, and $C_{i,j}$ are empirical constants chosen to match the experimental data. They are given in Table A2.

Vibration-Vibration Term

The VV term in the species Eq. (4) can be written as

$$VV_{i,v} = \sum_{j=1}^{N_d}\sum_{w=0}^{V_{max}} Q_{i,j,w,w+1}^{v+1,v}\{n_{i,v+1}n_{j,w}$$

$$- \exp[-(\Delta E_i^v - \Delta E_j^w)/kT]n_{i,v}n_{j,w+1}\} - Q_{i,j,w,w+1}^{v,v-1}$$

$$\times \{n_{i,v}n_{j,w} - \exp[-(\Delta E_i^{v-1} - \Delta E_j^w)/kT]n_{i,v-1}n_{j,w+1}\}$$

where $Q_{i,j,w-1,w}^{v,v-1}$ is the rate constant (in m^3/s) of the V-V transition:

$$X_i(v) + X_j(w-1) \rightarrow X_i(v-1) + X_j(w)$$

The rate constant is written as a sum of a short- and long-range contribution[1] as follows:

$$Q_{i,j,w-1,w}^{v,v-1} = Z_{i,j}(S_{i,j,w-1,w}^{v,v-1} + L_{i,j,w-1,w}^{v,v-1})$$

$$\times \exp[-(\Delta E_i^{v-1} - \Delta E_j^{w-1})/2kT]$$

Table A1 Spectroscopic constants

Species	ω_{ei}, cm^{-1}	$\omega_{ei}\chi_{ei}$, cm^{-1}	Θ_i, K	Ref.
CO-CO	2169.8	13.288	3121.0	13
N_2-N_2	2358.6	14.324	3396.8	13

Table A2 Vibration-translation

Species	$A_{i,j}$	$B_{i,j}$, $K^{1/3}$	$C_{i,j}$, $K^{2/3}$	$\alpha_{i,j}$, K^{-1}	Ref.
CO-CO	−15.23	280.5	−549.6	45.6×10^{-2}	15
CO-Ar	10.38	0.0	0.0	1.335×10^{-3}	15
CO-H_2	6.0001	−10.4149	−13.4749	3.4175×10^{-2}	9
CO-N_2	−7.934	147.7	0.0	3.295×10^{-2}	1
N_2-N_2	−12.539	258.9	−390.9	18.495×10^{-2}	1
N_2-Ar	10.38	0.0	0.0	1.335×10^{-3}	1

Table A3 Vibration-vibration

Species	$\mathscr{S}_{i,j}$, K^{-1}	$\mathscr{L}_{i,j}$, K	$b_{i,j}$, K	Ref.
CO-CO	1.64×10^{-6}	1.6142	40.36	15
CO-N_2	7.006×10^{-8}	1.897×10^{-2}	191.42	1
N_2-N_2	9.37×10^{-8}	0.0	—	1

with

$$Z_{i,j} = 4\sigma_{i,j}^2\sqrt{\pi kT/2\mu_{i,j}}$$

where $Z_{i,j}$ is the collision number in m^3/s, and $\pi\sigma_{i,j}^2$ is the collision cross section in m^2 with $\sigma = 3.75 \times 10^{-10}$ m. We also have

$$S_{i,j,w-1,w}^{v,v-1} = S_{i,j}T\frac{v}{1-\chi_{ei}v}\cdot\frac{w}{1-\chi_{ej}w}F(\lambda_{i,j,w-1,w}^{v,v-1})$$

$$L_{i,j,w-1,w}^{v,v-1} = \frac{\mathscr{L}_{i,j}}{T}\left(\frac{g_i^{v,v-1}}{g_i^{1,0}}\right)^2\left(\frac{g_j^{w-1,w}}{g_j^{1,0}}\right)^2 \cdot\exp\left[-\frac{(\Delta E_i^{v-1}-\Delta E_j^{w-1})^2}{b_{i,j}k^2T}\right]$$

where $\mathscr{S}_{i,j}$ (in K^{-1}), $\mathscr{L}_{i,j}$ in K, and $b_{i,j}$ in K, are empirical parameters fitted to available experimental data. Their values are given in Table A3. Also, $F(\lambda)$ is the same as before in the case of VT transfer, while the expression for λ now becomes

$$\lambda_{i,j,w-1,w}^{v,v-1} = 2^{-3/2}\sqrt{\frac{\Theta_{i,j}}{T}}\frac{|\Delta E_i^{v-1}-\Delta E_j^{w-1}|}{k\Theta_i}$$

Finally

$$\left(\frac{g_i^{v,v-1}}{g_i^{1,0}}\right)^2 = \left(\frac{a_i+1}{a_i+3-2v}\right)^2 \times\frac{v(a_i+2-2v)(a_i+4-2v)}{a_i(a_i+3-v)}$$

where $a_i = 1/\chi_{ei}$.

Spontaneous Radiative Decay Term

The SRD term in the species Eq. (4) for radiative transition between levels of the same electronic species can be written as[1]

$$\mathrm{SRD}_{i,v} = \sum_{w=1}^{w'}\mathscr{A}_i^{v+w,v}n_{i,v+w} - \mathscr{A}_i^{v,v-w}n_{i,v}$$

Table A4 Spontaneous radiative decay

Species	w'	$A^{1,0}$, 1/s	Ref.
CO-CO	4	30.3	15
N_2-N_2	—	0.0	1

where $\mathscr{A}$, the Einstein A coefficients, are given by

$$\frac{\mathscr{A}_i^{v,v-w}}{\mathscr{A}_i^{1,0}} = \frac{1}{(a_i-2)(a_i-3)}w\cdot\frac{v!}{(v-w)!} \times\frac{b_v(b_v+w)(b_v+2w)}{\prod_{q=0}^{w-1}(a_i-v+q)}$$

with $b_v = a_i - 2v - 1$, and w' and $\mathscr{A}_i^{1,0}$ (in 1/s) are given in Table A4.

Acknowledgments

This work was supported by the Air Force Office of Scientific Research under Grant AFOSR 91-0318. We also gratefully acknowledge Grant PAS 745-1 from the Ohio Supercomputer Center for the use of their Cray Y-MP. Helpful discussions with R. W. Briley of Mississippi State University are gratefully acknowledged.

References

[1]Chiroux de Gavelle de Roany, A., Flament, C., Rich, J. W., Subramaniam, V. V., and Warren, W. R., "Strong Vibrational Nonequilibrium in Supersonic Nozzle Flows," *AIAA Journal*, Vol. 31, No. 1, 1993, pp. 119–128.

[2]Hindmarsh, A. C., "LSODE and LSODI, Two Initial Value Ordinary Differential Equation Solvers," *ACM SIGNUM Newsletter*, Vol. 15, 1980, pp. 10, 11.

[3]Babu, V., Aithal, S., and Subramaniam, V. V., "On the Effects of Swirl in Arcjet Thruster Flows," 23rd International Electric Propulsion Conf., Paper IEPC-93-183, Seattle, WA, Sept. 1993.

[4]Briley, W. R., and McDonald, H., "Solution of the Multidimensional Compressible Navier-Stokes Equations by a Generalized Implicit Method," *Journal of Computational Physics*, Vol. 24, No. 4, 1977, pp. 372–397.

[5]Vincenti, W. G., and Kruger, C. H., *Introduction to Physical Gas Dynamics*, 2nd ed., Wiley, New York, 1965, pp. 108–110.

[6]Anderson, J. D., *Modern Compressible Flow with Historical Perspective*, 2nd ed., McGraw-Hill, New York, 1990, p. 59.

[7]Isaacson, E., and Keller, H. B., *Analysis of Numerical Methods*, 1st ed., Wiley, New York, 1966, pp. 58–61.

[8]Anderson, D. A., Tannehill, J. C., and Pletcher, R. H., *Computational Fluid Mechanics and Heat Transfer*, Hemisphere, McGraw-

Hill, New York, 1984, pp. 250, 251.

[9]Poulsen, L. L., and Billing, G. D., "Vibrational Deactivation of CO(v = 1) by p-H_2. The Importance of Higher-Order Multipole Moments," *Chemical Physics*, Vol. 89, No. 2, 1984, pp. 219–222.

[10]Straub, D. L., "Laser-Excited Chemical Vapor Deposition of Carbon on Silicon," M.S. Thesis, Ohio State Univ., Columbus, OH, 1991.

[11]Treanor, C. E., Rich, J. W., and Rehm, R. G., "Vibrational Relaxation of Anharmonic Oscillators with Exchange-Dominated Collisions," *Journal of Chemical Physics*, Vol. 48, No. 4, 1968, pp. 1798–1807.

[12]Briley, R. W., Buggeln, R. C., and McDonald, H., "Solution of the Three-Dimensional Navier-Stokes Equations for a Steady Laminar Horseshoe Vortex Flow," AIAA Paper 85-1520, 1985.

[13]Huber, K. P., and Herzberg, G., *Molecular Spectra and Molecular Structure, Vol. 4, Constants of Diatomic Molecules*, Van Nostrand Reinhold, New York, 1978.

[14]Yardley, J. T., *Introduction to Molecular Energy Transfer*, Academic Press, New York, 1980.

[15]Flament, C., et al., "Nonequilibrium Vibrational Kinetics of Carbon Monoxide at High Translational Mode Temperatures," *Chemical Physics*, Vol. 163, 1992, pp. 241–262.